Optical and Quantum Electronics (2022) 54: 658
https://doi.org/10.1007/s11082-022-04050-7

Reduction of effective material loss (EML) using decagonal photonic crystal fiber (D-PCF) for communication applications in the terahertz wave pulse

Md. Selim Hossain[1] · Shuvo Sen[2] · Md. Mahabub Hossain[3]

Received: 27 February 2022 / Accepted: 26 July 2022 / Published online: 29 August 2022

Abstract
We present an excellent design of five layers of decagonal shape in the cladding area and two elliptical shapes of core area based photonic crystal fiber (PCF) for many types of communiqué arenas in the THz wave pulse in this study. The Finite Element Method with perfectly matched layers used the optical parameters of our proposed D-PCF structure numerically to design and analyze. Therefore, D-PCF shows a low effective material loss of 0.0079 cm^{-1}, an increase in effective area of 3.49×10^{-8} m^2, a core power fraction of 85%, a low confinement and scattering loss, of 3.35×10^{-16} and 1.27×10^{-10} dB/km respectively at 1 THz of frequency. After analyses all the graphical results, our proposed D-PCF will be highly suitable for communiqué parts in the THz regions.

Keywords Low loss EML · Confinement loss · Effective area · Scattering loss · Optical communication

1 Introduction

Terahertz radiation which ranges from 0.1 to 10 THz, has recently sparked considerable interest due to its many applied submissions. The gray area exists within the situation of ultraviolet radioactivity and the microwave range. The huge THz occurrence has

This article is part of the Topical Collection on Photonics: Current Challenges and Emerging Applications.

Guest edited by Jelena Radovanovic, Dragan Indjin, Maja Nesic, Nikola Vukovic and Milena Milosevic.

✉ Md. Mahabub Hossain
im.mahabub@gmail.com

1 Department of Computing and Information System, Daffodil International University, Dhaka, Bangladesh

2 Department of Information and Communication Technology (ICT), Mawlana Bhashani Science and Technology University (MBSTU), Santosh, Tangail 1902, Bangladesh

3 Department of Electronics and Communication Engineering, Hajee Mohammad Danesh Science and Technology University, Dinajpur 5200, Bangladesh

applications in a variety of fields such as detection (Islam et al. 2017a, b), biomedical tomography (Hossain et al. 2021a), transport network (Pinto and Obayya 2007), bioengineering (Nagel et al. 2002), time-domain spectrometry (Vigneswaran et al. 2018), brininess (Amiri et al. 2018), infection sensor (Selim Hossain and Kamruzzaman , 2021), security screening (Islam et al. 2016a) applications. It also makes significant advances in the roots and documentation systems of the THz wave. The whole THz scheme is made up of three distinct parts: THz sources, wave guidance, and sensors. THz detector are commercially accessible. THz foundations and sensors are being quickly promoted with the help of advanced up-to-date expertise. The most important THz sources are Gunn diodes, free-electron lasers, quantum lasers, biological gas far-infrared lasers, and so on. Furthermore, the most useful T-ray detectors are bolometers, Golay cells, pyroelectric detectors, and Schottky barrier diodes. Most THz waveguides, however, rely heavily on free-space wave proliferation due to frequency propagation. However, here are some issues with free space wave proliferation, such as path loss, material loss, and high absorption loss. Researchers had previously proposed numerous waveguides to mitigate these issues. Bragg fibers (Jeon et al. 2005), metallic waveguides (Wang and Mittleman 2004), silver coated hollow glass (Bowden et al. 2007; Skorobogatiy and Dupuis 2007), subwavelength waveguides (Hassani et al. 2008), parallel-plate waveguides (Chen et al. 2006), and so on are examples. Metallic waveguides used in THz transmission can encounter issues such as high winding loss and frequency-dependent losses. Bragg fibers are more efficient in diffusion and riddling submissions. Nonetheless, using Bragg fibers to achieve desirable output in applied wavelength division multiplexing submissions is difficult. The main limitation of a parallel-plate waveguide is confinement loss.

Microstructure core PCF has newly demonstrated progressive physical elasticity and extremely high optical possessions. One important gain is that determined optical power permits through the core region, which aids to decrease material loss. Two basic optical managerial possessions are usually originated in microstructure core PCF: modified total internal reflection (MTIR) and photonic bandgap (PBG). When the RI of the cladding is better than the core RI, the photonic bandgap function operates in PCF. When the core RI exceeds the cladding, the MTIR impact is activated. Microstructure PCF is proposed as a THz supervisory standard to attain lower confinement loss, high numerical aperture, lower dispersion, high birefringence, and better waveguiding properties. PCF suffers from material losses due to the use of solid materials in the core region. A porous air core is favored athwart a solid body (Tang et al. 2013a). Such properties make it possible to use porous polymer PCFs in a variety of filtering and sensing submissions. Other kinds of circumstantial resources, such as ZEONEX, TOPAS, Teflon, Polymethyl methacrylate, and ZBLAN (Yuan et al. 2011; Bulbul et al. 2020; Hossain et al. 2021b; Jiang et al. 2015; Dash and Jha 2014), are secondhand to improve optical guiding properties and reduce EML. ZEONEX has been used as the contextual material since it has excellent optical possessions such as low material loss, high temperature insensitivity, and low dispersion (Hossain et al. 2021c).

In past years, low loss THz waveguides are discussed briefly by many researchers. Porous core-based PCF was described by Hasanuzzaman et al. (Hasanuzzaman et al. 2015) and presented the higher effective EML of 0.035 $cm^{-1.}$ Hasan et al. (Hasan et al. 2016) discussed a square lattice photonic crystal fiber and reported an EML of 0.076 $cm^{-1.}$ Islam et al. (Islam et al. 2016b) showed their structure such as porous core-based PCF and found an EML of 0.050 $cm^{-1.}$ Sen et al. (Md. Selim Hossain, Nazmul Hussain, Zakir Hossain, Md. Sakib Zaman, Md. Navid Hasan Rangon, Md. Abdullah-Al-Shafi, Shuvo Sen, Mir Mohammad Azad, Performance analysis of alcohols sensing with optical sensor procedure using circular photonic crystal fiber (C-PCF) in the terahertz regime, Sensing and

Bio-Sensing Research, Volume 35 2022) showed the polymer-based photonic crystal fiber and their results of an EML of 0.040 cm^{-1}. After checking the previous structure (Hasanuzzaman et al. 2015; Hasan et al. 2016; Islam et al. 2016b; Md. Selim Hossain, Nazmul Hussain, Zakir Hossain, Md. Sakib Zaman, Md. Navid Hasan Rangon, Md. Abdullah-Al-Shafi, Shuvo Sen, Mir Mohammad Azad, Performance analysis of alcohols sensing with optical sensor procedure using circular photonic crystal fiber (C-PCF) in the terahertz regime, Sensing and Bio-Sensing Research, Volume 35 2022; ; ; ;;;), we get a good chance to develop a new structure by removing very low losses for communication applications.

Our D-PCF is an arrangement of five layers of decagonal form within the covering area and two elliptical forms of photonically crystal (D-PCF) core area of various types of communication in the terahertz belt. This D-PCF displays a low EML of 0.0079 cm^{-1} following an examination of numerical findings; a large effective area of 3.49×10^{-8} m^2; a core power fraction (CPF) of 85%, a low CL and SL of as 3.35×10^{-16} dB/m and 1.27×10^{-10} dB/km at 1 THz respectively.

2 Design methodology of D-PCF

Figure 1 depicts structural cross sections such as (a) Decagonal cladding regions, (b) Elliptical core regions, and (c) Mode field distribution. In this case, the diameter and pitch at the cladding areas are signified by the constraints d_1 and A_1. The constraints d_1/A_1 is called the air filling proportion which is to watch in contradiction of collapse between two air holes in the cladding area. The parameters of A_c, d_a, and d_b are indicated at the core area by the pitch and distances of the two elliptical AHs. The ZEONEX material was used to remove the EML, confinement loss (CL), and Scattering loss (SL) in this case. Here, the optimum cladding

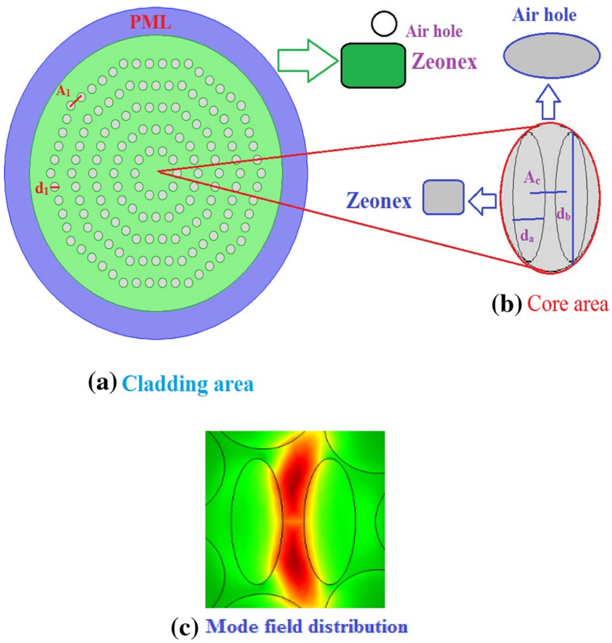

Fig. 1 Designed sights of D-PCF fiber, **a** Cladding area **b** Elliptical core area **c** Mode field distributions for both x and y polarization at the frequency of 1 THz

diameter is 282 μm, cladding pitch of 345 μm, diameter of core $d_a = 70$ μm, $d_b = 160$ μm, core pitch $\Lambda_c = 100$ μm and $PML_1 = 2250$ μm and $PML_2 = 2450$ μm.

3 Mathematical analysis of optical properties

It has been known to us that a large EA-based PCF fiber shows a low EML. Here, the EA is calculated the following equation (Ren et al. 2012):

$$A_{ea} = \frac{\left[\int I(e)ede\right]^2}{\left[\int I^2(e)de\right]^2} \tag{1}$$

where, A_{ea} is the effective area and intensity of electric field is the $I(e) = |E_e|^2$.

PF is indicated that the most amount of power flowing in the core area of the D-PCF structure. Here, Power fraction is determined by the following equation (Luo et al. 2017):

$$\eta = \frac{\int_i S_{zt} dAt}{\int_{all} S_{zt} dAt} \tag{2}$$

where S_{zt} is area of interest such as cladding, core, or air hole is indicated by nominator integration and the entire cross-section area is denoted by denominator integration.

V-parameter displays the single mood communication and the V-parameter is shown the following equation (Islam et al. 2016c):

$$V = \frac{2\pi ef}{c}\sqrt{ne_{coe}^2 - ne_{cle}^2} \le 2.045 \tag{3}$$

where, the core and cladding area based effective mood index is defined by the n_{coe} and n_{cle} and c is the radius of the core.

The CL is a vital aspect of D-PCF structure and this CL (L_{ce}) is shown by Islam et al. 2017c:

$$L_{ce} = 8.686 \times K_0 \,\mathrm{Im}\left[n_{ea}\right](\mathrm{dB/m}) \tag{4}$$

where, the free wave number is $K_0 = \left(\frac{f}{c}\right)$, c is the speed of photon, frequency is f and the imaginary part of ERI is $\mathrm{Im}\left[n_{ea}\right]$.

The SL is well-defined with the total amount of loss of the D-PCF structure. At this time, the scattering loss is calculated by Ahmed et al. 2017a:

$$\alpha_S = C_S \times \left(\frac{f}{c}^4\right)(\mathrm{dB/km}) \tag{5}$$

where, the scattering coefficient is C_S.

The background material of Zeonex creates a very low EML and this EML is calculated by Rana et al. (2014):

$$\alpha_{ea} = \sqrt{\frac{\varepsilon_0}{\mu_0}}\left(\frac{\int \mathrm{mat}^{n}\mathrm{mat}|E|^{2\alpha}\mathrm{mat}^{dAt}}{\left|\int_{all} S_{zt} dAt\right|}\right)(\mathrm{cm}^{-1}) \tag{6}$$

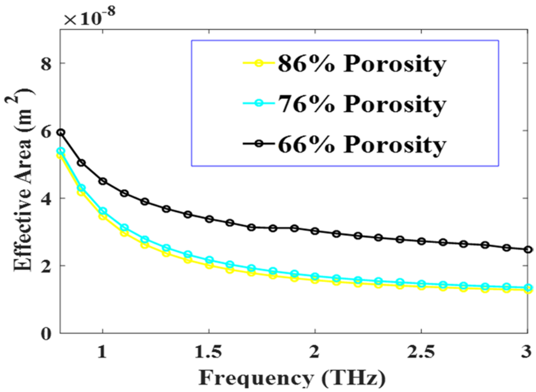

Fig. 2 Calculation of effective area along with the frequencies

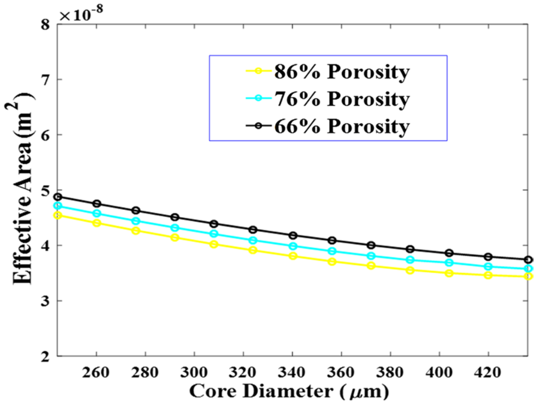

Fig. 3 Calculation of Effective area in accordance with the core diameters

where, the relative permittivity and the permeability of free space are denoted by ε_0 and μ_0, the RI of the material is n_{mat} and bulk material absorption loss is α_{mat}.

3.1 Simulated results and discussions

We chose the optimum porosity of 86, 76, and 66% because it is clear from Figs. 2, 3, 4, 5, 6, 7, 8, 9 that the total light transmits inside the CA. This D-PCF fiber exhibits improved graphic outputs for optical possessions such as low EML, low SL, larger EA, high core power fraction, better V-parameter, and low CL with frequency ranges; ranging from 0.08 to 3 THz.

In Fig. 2, the EA is decreasing with the frequency varieties from 0.80 to 3 THz for three porosities for such as 66, 76, and 86%. At 1 THz frequency of optimum parameters for 86, 76, and 66% porosities, the EA is determined of 3.49×10^{-8}, 3.60×10^{-8}, and 4.55×10^{-8} m^2 respectively.

Here, EA is slightly decreased with the core diameters from $D_{core}=280$ μm to $D_{core}=440$ μm for three porosities for such as 66, 76, and 86% in Fig. 3. At 1 THz frequency of optimum parameters for 86, 76, and 66% porosities, the EA is determined as 4.27×10^{-8}, 4.55×10^{-8}, and 4.63×10^{-8} m^2.

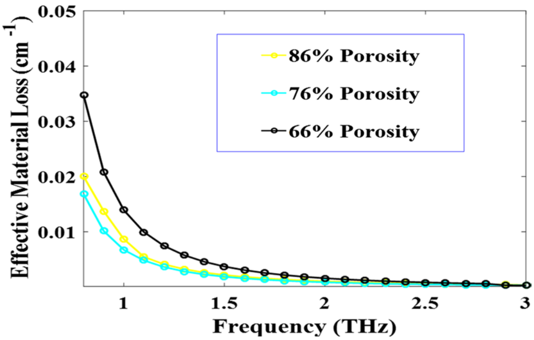

Fig. 4 Measurement of EML with respect to the frequencies

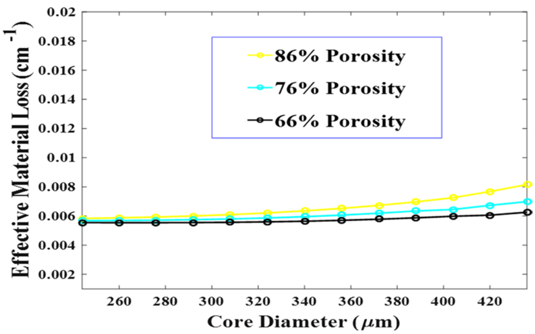

Fig. 5 Presentation of EML with the core diameters

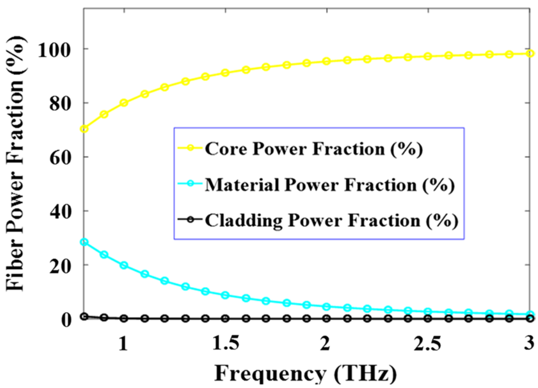

Fig. 6 Core power with respect to the frequencies for the core, cladding, and materials values of 85, 0.25, and 21% respectively

In Fig. 4, the EML is a very decreasing with the frequency assortments from 0.80 to 3 THz for three porosities for such as 66, 76, and 86%. At 1 THz frequency of optimum parameters for 86, 76, and 66% porosities, the EML is measurement of 0.0079 cm^{-1}, 0.0069 cm^{-1} and 0.0127 cm^{-1}.

In these graphical results, the EML is slightly increased with the core diameters from D_{core} = 280 μm to D_{core} = 440 μm for three porosities for such as 66, 76, and 86%. At 1 THz frequency of optimum parameters for 86, 76, and 66% porosities and optimum core diameter D_{core} = 420 μm, EML is calculated 0.0079 cm^{-1}.

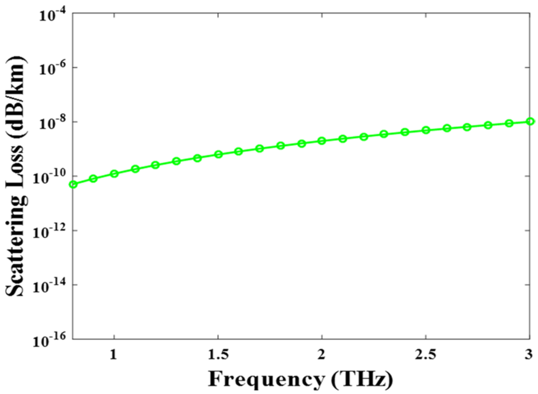

Fig. 7 Graphical representation of scattering loss with respect to the frequencies

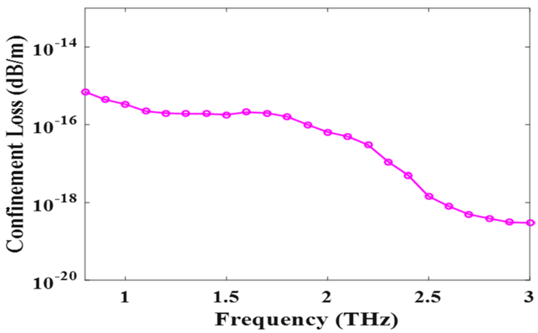

Fig. 8 Presentation of CL along with the frequencies

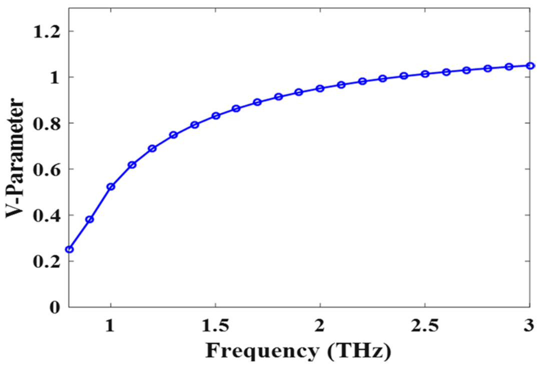

Fig. 9 Calculation of V-parameter along with the frequencies

Figure 6 displays that the PF of the core, cladding, and materials has good relationships with frequency ranges; ranging from 0.80 to 3 THz. The majority of the light passes through the core area, while some power is lost in the cladding and materials areas. Optimum values are $D_{core} = 420$ µm, 85, 0.25, and 21% of core, cladding, and materials of the power fraction respectively which has been found at 1 THz.

In Fig. 7, the SL is slightly growing with the frequency ranges from 0.80 to 3 THz. For 86% porosity and 1 THz frequency, the SL is at 1.27×10^{-10} dB/km.

Table 1 Optical properties among the proposed D-PCF and other reported PCFs

References	EML (cm^{-1})	Porosity (%)	Power fraction	Confinement loss (dB/m)	Effective area ($A_{eff}(m^2)$)
Ahmed et al. (2017b)	0.047	–	54%	–	2.42×10^{-07}
Luo et al. (2017)	0.081	–	46.9%	1.96×10^{-03}	1.24×10^{-03}
Paul et al. (2019a)	0.1	–	57.50%	1.38×10^{-12}	1.1×10^{-05}
Paul and Ahmed (2020)	0.038	74	56%	2.35×10^{-01}	6.75×10^{-05}
Islam et al. (2016c)	0.110	–	–	–	0.98×10^{-07}
Proposed D-PCF	0.0079	86	85%	3.35×10^{-16}	3.49×10^{-8}

In Fig. 8, the confinement loss (CL) is decreasing with the frequency ranges from 0.80 to 3 THz. For 86% porosity and 1 THz frequency, confinement loss (CL) is the order of 3.35×10^{-16} dB/m.

In this graphical Fig. 9, the V-parameter is increasing from 0.80 to 3 THz and this V-parameter shows single mood communication system ($V-\text{parameter} \le 2.045$). Here, the optimum cladding diameter is 282 µm, cladding pitch of 345 µm, diameter of core $d_a = 70$ µm,$d_b = 160$ µm and core pitch $\Lambda_c = 100$ µm.

In Table 1, the projected D-PCF has EML is 0.0079 cm^{-1}, a larger EA of 3.49×10^{-8} m^2, CPF of 85%, and a low CL of 3.35×10^{-16} dB/m than other reported PCFs.

Here, fabrication is an important way to fabricate the photonic crystal fiber. Many advanced fabrication techniques such as stack and draw, tube stacking drilling, sol–gel (Ahmed et al. 2017a; Rana et al. 2014; Paul et al. 2019b; Islam et al. 2017d; Tang et al. 2013b) can be considered, however the sol–gel (Hamzaoui et al. 2012; Hasan et al. 2017; Bao et al. 2012; Nielsen et al. 2009; Ponseca et al. 2008) process will be appropriate to manufacture the proposed D-PCF.

4 Conclusion

In this study, a decagonal (D-PCF) photonic crystal fiber was examined using PML and the FEM based COMSOL Multiphysics software tool for communication network performance analysis. In addition, we used ZEONEX as a background material to remove EML, CL, and SL. After reviewing all of the graphical results, we discovered that our D-PCF has an EML, a large effective area, a core power fraction, and a low CL and SL of 0.0079 cm^{-1}, 3.49×10^{-8} m^2, 85%, 3.35×10^{-16} dB/m and 1.27×10^{-10} dB/km correspondingly at 1 THz frequency range. So, our D-PCF is proper for communication parts in the THz regions.

Acknowledgements The authors are grateful to the participants who contributed to this research. The authors have not received any funding for this research.

Declarations

Conflict of interest The authors declare that they have no competing of interest.

References

Ahmed, K., Chowdhury, S., Paul, B.K., Islam, M.S., Sen, S., Islam, M.I., et al.: Ultrahigh birefringence, ultralow material loss porous core single-mode fiber for terahertz wave guidance. Appl Opt **56**(12), 3477–3483 (2017a). https://doi.org/10.1364/AO.56.003477

Ahmed, K., Islam, M., Sen, S., Paul, B.K., Chowdhury, S., Hasan, M., Uddin, M.S., Asaduzzaman, S., Bahar, A.N.: Low-loss single mode terahertz microstructure fiber with near-zero-flattened dispersion. Adv. Sci. Eng. Med. **9**(10), 829–836 (2017b)

Amiri, I.S., Paul, B.K., Ahmed, K., Aly, A.H., Zakaria, R., Yupapin, P., Vigneswaran, D.: Tri-core photonic crystal fiber based refractive index dual sensor for salinity and temperature detection. Microw. Opt. Technol. Lett. (2018)

Bao, H., Nielsen, K., Rasmussen, H.K., Jepsen, P.U., Bang, O.: Fabrication and characterization of porous-core honeycomb bandgap THz fibers. Opt. Express **20**(28), 29507–29517 (2012)

Bulbul, A.A.-M., Imam, F., Awal, Md. A., Mahmud, M.A.P.: A novel ultra-low loss rectangle-based porous-core pcf for efficient THz Waveguidance. Des. Numer. Anal.. Sens. **20**(22), 6500 (2020)

Bowden, B., Harrington, J.A., Mitrofanov, O.: Silver/polystyrenecoated hollow glass waveguides for the transmission of terahertz radiation. Opt. Lett. **32**(20), 2945–2947 (2007)

Chen, L., Chen, H., Kao, T., Lu, J., Sun, C.: Low-loss subwavelength plastic fiber for terahertz wave guiding. Opt. Lett. **31**(3), 308–310 (2006)

Dash, J.N., Jha, R.: Graphene-based birefringent photonic crystal fber sensor using surface plasmon resonance. IEEE Photon. Technol. Lett. **26**(11), 1092–1095 (2014)

El Hamzaoui, H., Ouerdane, Y., Bigot, L., Bouwmans, G., Capoen, B., Boukenter, A., Girard, S., Bouazaoui, M.: Sol-gel derived ionic copper-doped microstructured optical fiber: a potential selective ultraviolet radiation dosimeter. Opt. Express **20**(28), 29751–29760 (2012)

Hasan, M.R., Islam, M.A., Rifat, A.A.: A single mode porous-core square lattice photonic crystal fiber for THz wave propagation. J Eur Opt Soc-Rap Pub **12**(1), 15 (2016)

Hasan, M.R., Akter, S., Khatun, T., Rifat, A.A., Anower, M.S.: Dual-hole unit-based kagome lattice microstructure fiber for low-loss and highly birefringent terahertz guidance. Opt. Eng. **56**(4), 043108 (2017)

Hasanuzzaman, G.K.M., Habib, M.S., Razzak, S.A., Hossain, M.A., Namihira, Y.: Low loss single-mode porous-core kagome photonic crystal fiber for THz wave guidance. J Light Tech **33**(19), 4027–4031 (2015)

Hassani, A., Dupuis, A., Skorobogatiy, M.: Porous polymer fibers for low-loss terahertz guiding. Opt. Express **16**(9), 6340–6351 (2008)

Hossain, M.S., Sen, S., Hossain, M.M.: Performance analysis of octagonal photonic crystal fiber (O-PCF) for various communication applications. Phys Scr. **96**(5), 55506 (2021a). https://doi.org/10.1088/1402-4896/abe323

Hossain, M.S., Hasan, M.M., Sen, S., Mollah, M.S.H., Azad, M.M.: Simulation and analysis of ultra-low material loss of single-mode photonic crystal fiber in terahertz (THz) spectrum for communication applications. J. Opt. Commun., **4873** (2021b). Doi: https://doi.org/10.1515/joc-2020-0224.

Hossain, M.S., Sikder, A.S., Sen, S., et al.: Design and numerical analysis of Zeonex-based photonic crystal fiber for application in different types of communication networks. J Comput Electron (2021c). https://doi.org/10.1007/s10825-021-01704-9

Hossain, M.S., Hussain, N. Hossain, Z., Zaman, M.S., Hasan Rangon, M.N., Abdullah-Al-Shafi, M., Sen, S., Azad, M.M.: Performance analysis of alcohols sensing with optical sensor procedure using circular photonic crystal fiber (C-PCF) in the terahertz regime. Sens. Bio Sens. Res. **35**, 100469. ISSN 2214–1804 (2022). https://doi.org/10.1016/j.sbsr.2021.100469

Islam, S., Rana, S., Islam, M.R., Faisal, M., Rahman, H., Sultana, J.: Porous core photonic crystal fiber for ultra-low material loss in THz regime. IET Commun., **10**(16), 2179–2183, (2016a).

Islam, M.S., Rana, S., Islam, M.R., Faisal, M., Rahman, H., Sultana, J.: Porous core photonic crystal fibre for ultra-low material loss in THz regime. IET Com **10**(16), 2179–2183 (2016b)

Islam, R., Habib, M.S., Hasanuzzaman, G.K.M., Rana, S., Sadath, M.A., Markos, C.: A novel low-loss diamond-core porous fiber for polarization maintaining terahertz transmission. IEEE Photon Technol Lett **28**(14), 1537–1540 (2016c)

Islam, M.I., Ahmed, K., Asaduzzaman, S., Paul, B.K., Bhuiyan, T., Sen, S., Islam, M.S., Chowdhury, S.: Design of single mode spiral photonic crystal fiber for gas sensing applications. Sens. Bio Sens. Res., **13**, 55–62, (2017a).

Islam, M.I., Ahmed, K., Sen, S., Chowdhury, S., Paul, B.K., Islam, M.S., Asaduzzaman, S.: Design and optimization of photonic crystal fiber-based sensor for gas condensate and air pollution monitoring. Photonic Sens **7**(3), 234–245 (2017b)

Islam, M.S., Sultana, J., Rana, S., Islam, M.R., Faisal, M., Kaijage, S.F., Abbott, D.: Extremely low material loss and dispersion flattened TOPAS based circular porous fiber for long distance terahertz wave transmission. Opt. Fiber Technol. **34**, 6–11 (2017c). https://doi.org/10.1016/j.yofte.2016.11.014
Islam, M.S., Sultana, J., Atai, J., Abbott, D., Rana, S., Islam, M.R.: Ultra lowloss hybrid core porous fiber for broadband applications. Appl. Opt. **56**(9), 1232–1237 (2017d)
Jeon, T.I., Zhang, J., Grischkowsky, D : THz Somerfeld wave propagation on a single metal wire. Applied Phys. Lett., **86**(16), 161904, (2005)
Jiang, X., Joly, N.Y., Finger, M.A., Babic, F., Wong, G.K., Travers, J.C., Russell, P.S.J.: Deep-ultraviolet to mid-infrared super continuum generated in solidcore ZBLAN photonic crystal fiber. Nat. Photonics **9**(2), 133–139 (2015)
Luo, J., Tian, F., Qu, H., Li, L., Zhang, J., Yang, X., Yuan, L.: Design and numerical analysis of a THz square porous-core photonic crystal fiber for low flattened dispersion, ultrahigh birefringence. Appl. Opt. **56**, 6993–7001 (2017). https://doi.org/10.1364/AO.56.006993
Md. Selim Hossain, M.M. Kamruzzaman, S.S., Azad, M.M., Mollah, M.S.H.: Hexahedron core with sensor based photonic crystal fiber: An approach of design and performance analysis. Sens. Bio Sens. Res (2021). Doi: https://doi.org/10.1016/j.sbsr.2021.100426
Nagel, M., Bolivar, P.H., Brucherseifer, M., Kurz, H., Bosserhoff, A., Büttner, R.: Integrated THz technology for label-free geneticdiagnostics. Appl. Phys. Lett. **80**(1), 154–156 (2002)
Nielsen, K., Rasmussen, H.K., Adam, A.J., Planken, P.C., Bang, O., Jepsen, P.U.: Bendable, low-loss Topas fibers for the terahertz frequency range. Opt. Express **17**(10), 8592–8601 (2009)
Paul, B.K., Haque, M., Ahmed, K., Sen, S.: A novel hexahedron photonic crystal fiber in terahertz propagation: design and analysis. Photon. **6**, 32–38 (2019a)
Paul, B.K., Bhuiyan, T., Abdulrazak, L.F., Sarker, K., Hassan, M.M., Shariful, S., Ahmed, K.: extremely low loss optical waveguide for terahertz pulse guidance. Res. Phys. **15**, 102666 (2019b)
Paul, B.K., Ahmed, K.: Analysis of terahertz waveguide properties of Q-PCF based on FEM scheme. Opt Mater **100**, 109634 (2020)
Pinto, D., Obayya, S.S.A.: Improved complex envelope alternative direction implicit finite difference time domain method for photonic bandgap cavities. IEEE J. Lightwave Technol. **25**(1), 440–447 (2007)
Ponseca, C.S., Jr., Pobre, R., Estacio, E., Sarukura, N., Argyros, A., Large, M.C., van Eijkelenborg, M.A.: Transmission of terahertz radiation using a microstructured polymer optical fiber. Opt. Lett. **33**(9), 902–904 (2008)
Rana S., Hasanuzzaman G.K., Habib S., Kaijage S.F., Islam R.: Proposal for a low loss porous core octagonal photonic crystal fiber for T-ray wave guiding. Opt. Eng. **53**(11):115107–115107. Doi: https://doi.org/10.1117/1.OE.53.11.115107(2014)
Ren, H-Z., Guo, P.,Yang, LF. The numerical calculation on the effective area of photonic crystal fiber using FEM. Adv. Mater. Res **468471**, 2417–2422 (2012). Doi: https://doi.org/10.4028/www.scientific.net/amr.468-471.2417.
Skorobogatiy, M., Dupuis, A.: Ferroelectric all-polymer hollow Bragg fibers for terahertz guidance. Appl. Phys. Lett. **90**(11), 113514 (2007)
Tang, X., Jiang, Y., Sun, B., Chen, J., Zhu, X., Zhou, P., Wu, D., Shi, Y.: IEEE Photonics Technol. Lett. **25**, 331 (2013a)
Tang, X., Jiang, Y., Sun, B., Chen, J., Zhu, X., Zhou, P., Wu, D., Shi, Y.: Elliptical hollow fiber with inner silver coating for linearly polarized terahertz transmission. IEEE Photonics Technol. Lett. **25**(4), 331–334 (2013b)
Vigneswaran, D., Ayyanar, N., Sharma, M., Sumathi, M., Rajan, M., Porsezian, K.: Salinity sensor using photonic crystal fber. Sens. Actuators A Phys. **269**, 22–28 (2018)
Wang, K., Mittleman, D.M.: Metal wires for terahertz waveguiding. Nature **432**, 376–379 (2004)
Yuan, W., Khan, L., Webb, D.J., K. Kalli, K., Rasmussen, H. K., Stefani, A., Bang O.: Humidity insensitive TOPAS polymer ber Bragg grating sensor. Opt. Express, **19**(20), 19731–19739 (2011)